

Correlation in low-dimensional electronic states on metal surfaces

A Menzel, Zh Zhang¹, M Minca, Th Loerting, C Deisl and E Bertel

Institute of Physical Chemistry, University of Innsbruck, Austria

E-mail: Alexander.Menzel@uibk.ac.at

New Journal of Physics 7 (2005) 102

Received 1 December 2004

Published 29 April 2005

Online at <http://www.njp.org/>

doi:10.1088/1367-2630/7/1/102

Abstract. We investigate quasi-one-dimensional (quasi-1D) surface states on metals as a well-defined model system for the study of correlation effects by angle-resolved photoemission. Both dimensionally constrained Shockley and Tamm states are examined, the former on the striped O/Cu(1 1 0) phase, the latter on Pt(1 1 0) with and without adsorbates. We observe an unusual change in photoemission intensity of quasi-particle peaks as a function of temperature or adsorbate coverage, which is very similar to ARUPS results on layered systems, Kondo systems, Mott-insulator systems and high- T_c superconductors. The intensity change of the quasi-particle peak is interpreted in terms of a coherent–incoherent transition of the quasi-1D states. For the Tamm states on Pt(1 1 0), we also find other typical fingerprints of correlation such as a kink in the dispersion and a significant mass renormalization close to E_F . A saddle point at the Fermi level provides a large density of states. Therefore, it is reasonable to expect that this quasi-1D surface resonance is involved in surface phase transitions. The results support our previous report about a surface charge-density-wave-induced phase transition on Br/Pt(1 1 0).

Contents

1. Introduction	2
2. Experimental setup	4
3. Results and discussion	5
Acknowledgments	17
References	17

¹ Present address: Department of Chemistry, University of Texas at Austin, USA.

1. Introduction

A hallmark of correlated electronic systems is their propensity to phase instabilities [1]. This is due to the delicate balance between various interactions, which can be easily tipped into one or the other direction by small changes of control parameters. As an example, we show in figure 1 a schematic phase diagram generic for the quasi-one-dimensional (quasi-1D) Bechgaard salts [2], but in a global way characteristic for a multitude of correlated systems. It displays a variety of phases which can be reached for instance by changing the external pressure, by varying the carrier concentration via doping, or by changing the structure via chemical substitution. The phase diagram shown in figure 1 is technologically extremely interesting, be it for the presence of a superconducting phase, the antiferromagnetic phase or the Mott metal–insulator transition. Yet, the interactions in correlated systems, which govern all these phase transitions, are not thoroughly understood. It is therefore rather important to gather experimental information on correlation effects. Angle-resolved photoemission spectroscopy (ARUPS), in particular on high- T_c superconductors, has played a key role in recent advances of our understanding [3]. A major obstacle in such studies is the complicated structure of the—mainly oxidic—compounds studied in this context. A notorious example is the long-standing discussion about the peak-dip-hump feature in $\text{Bi}_2\text{Sr}_2\text{CaCu}_2\text{O}_{8-\delta}$ [4]. Surface and bulk are expected to behave differently in correlated compounds due to the different coordination, and this, too, tends to obscure the characteristic spectral features [5, 6]. Finally, long-range effects are intrinsic to correlated systems and low-dimensional electronic states, hence even small defect concentrations can trigger instabilities and change the behaviour of the ideal system [7].

In view of these complications, it appears highly desirable to study correlation effects on model systems, preferably surface systems, which would eliminate the ambiguity with respect to bulk and surface effects. Furthermore, such model systems should exhibit a simple structure, a low defect concentration and a low cross-section for beam-damage. All these requirements can be met to a large extent by 1D structures on metal surfaces. Metal surfaces can be prepared with very low defect density. The metallic substrate makes the system rather insensitive to beam-induced damage and dimensionally confined electron states are expected to exhibit substantial correlation effects.

A key question, which partly motivated the present study, is of course whether the coupling to the semi-infinite Fermi liquid of the substrate can be sufficiently suppressed to avoid the quenching of all interesting correlation effects, in particular the associated phase instabilities. A second question to be discussed is how to extract the information about correlation from ARUPS. A standard, though by no means trivial, procedure is to extract the real and imaginary part of the self-energy from the spectral function. Both the renormalization of the electron effective mass close to E_F (the so-called kink feature) and as the deviation from the ω^{-2} dependence of the lifetime expected for Fermi liquids may be taken as indicators of correlation. Furthermore, correlation is intimately related to the degree of localization of electrons. Emission from 2D or 3D Bloch states normally gives rise to quasi-particle (QP) peaks in the photoemission spectra with the possible exception of features close to E_F which derive from electron–phonon coupling. The situation is different for 1D or 0D electron states. For strictly 1D electron states, a Luttinger liquid behaviour is expected, which means a complete breakdown of the QP concept [8]. New excitations arise separately in the spin and the charge system. It is not clear whether Luttinger liquid behaviour has been really observed in photoemission so far [9]–[11]. Strong electron–phonon coupling, which is also prevalent in 1D systems, tends to obscure the spin–charge

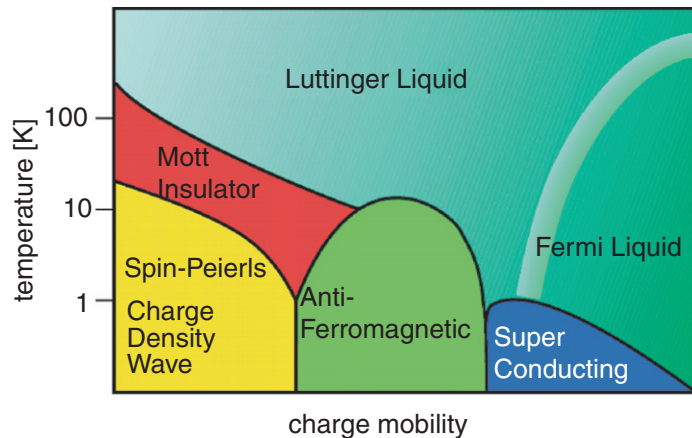


Figure 1. Schematic phase diagram of a prototypical low-dimensional electronic system. The charge mobility can be modified by external pressure, doping, changes of the chemical composition, etc [2].

separation [12]. In fact, real 1D or quasi-1D systems are expected to be unstable against Peierls transitions [12]–[15]. Increasing electron localization has still another effect on the photoemission spectra: as long as the low-dimensional electron states overlap to a sufficient extent, they are phase-coherent and give rise to QP features in the spectra. With increasing localization, however, the overlap decreases and eventually the phase coherence is destroyed. As a consequence, the final state photo-hole can be considered as a localized excitation and the spectral weight is shifted from a QP feature to an incoherent peak. Conceptually, the coherent–incoherent transition can be brought about by different mechanisms. A possible scenario is the thermal disorder causing local deviations ΔU from the strictly periodic lattice potential. If ΔU becomes larger than the bandwidth W , an Anderson-localized, incoherent state evolves [16]–[18]. Alternatively, localization of the electrons increases their Coulomb interaction U and if U exceeds W , a Mott transition takes place [5]. Still another example of coherent–incoherent transitions is provided by Kondo systems. Here the ground state is formed by a hybrid wavefunction containing the localized (‘impurity’) level, which originally carries the magnetic moment, and delocalized states from the conduction band manifold. This ground state is a singlet state. The corresponding triplet states are slightly higher in energy, but due to the Pauli principle there is no hybridization possible with the conduction band states. The triplet states are associated with the localized impurity level only. In the simplest model, the singlet–triplet energy splitting scales with the square of the hybridization matrix element V or, equivalently, with the antiferromagnetic exchange coupling J [19]. At low temperature, only the ground state is populated and photoemission yields a coherent QP peak. At $T > T_{\text{Kondo}}$, the triplet states are thermally populated and a spectral-weight transfer from the QP peak to incoherent features takes place in photoemission [20]. It appears that similar coherent–incoherent transitions occur in layered systems as transitions from 3D to 2D behaviour [21]. In high- T_c superconductors such a transition coincides with the superconducting transition [22], but it is not yet entirely clear whether it is a 3D to 2D or a 2D to 1D transition [23, 24]. Actually, it is also conceivable that the breakdown of 3D phase coherence could trigger the charge separation into stripes. In this case, the transition should be designated as 3D to 1D transition. From this discussion and the experimental examples cited above, it becomes clear that the temperature evolution of QP peaks, namely the spectral-weight transfer from coherent to incoherent photoemission peaks as a function of temperature, is also a hallmark of correlated systems.

In the present study, we investigate quasi-1D states on metal surfaces by angle-resolved photoemission and search for evidence of correlation in these systems. The first example is the Cu(1 1 0) surface. Here, a Shockley surface state is found at the \bar{Y} point of the surface Brillouin zone (SBZ) [25]. The discovery of the striped surface oxide phase O/Cu(1 1 0) [26] offers the exciting possibility to constrain the surface state into the narrow clean Cu channels between the surface oxide stripes. At low oxygen coverages, the oxide stripe width is small and allows for interaction between the stripes. The structure can then be envisioned as a lateral super-lattice and can be modelled by a Kronig–Penney potential [27]. The coupling between the stripes is sufficient to ensure coherent behaviour at low temperatures and correspondingly QP peaks are observed. At larger O coverages, the broader oxide barriers reduce the coupling and coherence is lost. The QP peaks disappear and instead the ARUPS features can be interpreted as incoherent emission from individual quantum well states. The same transition, however, may be brought about at low oxide barrier width by increasing the temperature [18]. While this provides a clear example of a coherent–incoherent transition, it is not very well suited to study effects of strong correlation, such as correlation-induced phase transitions. The reason is the extremely small charge density associated with the Cu(1 1 0) \bar{Y} surface state, which amounts to only a few per cent of an electron per surface atom. An additional, more technical problem is the control of the stripe width. As the channels become smaller and thereby approach the 1D limit, even small variations in the channel width act as increasingly strong perturbation of the perfectly periodic potential.

One can expect to observe the interesting ground state properties associated with correlation, such as phase instabilities, only if the surface state band produces a large density of states (DOS) at E_F . Therefore, d derived surface states are more promising candidates. An obvious choice is to search for such Tamm states on the strongly anisotropic fcc(1 1 0) surfaces. In particular the d^9 transition metals are interesting in this respect, because a Tamm state split from the top of the d bands should straddle the Fermi level. We choose the Pt(1 1 0) surface for the additional reason of the (1×2) missing-row reconstruction, which yields more or less isolated, close-packed atom chains with a separation of 7.84 Å. This is large enough to allow an interaction of d orbitals only through coupling with the substrate. Furthermore, Pt linear chain compounds, such as the tetracyanoplatinate complexes are well known to exhibit charge separation [28]. Even the groundstate of bulk Pt is close to electronic instabilities. The absence of superconductivity at normal conditions is attributed to ferromagnetic fluctuations [29]. A single Fe impurity is known to polarize ~ 100 Pt atoms [30]. The existence of a charge density wave (CDW) instability has been invoked as a possible explanation for scanning tunnelling microscopy (STM) observations on the Pt(1 0 0) surface [31]. An STM investigation of the halogenated Pt(1 1 0) surface by our group revealed a phase transition just above $\Theta_{\text{Halogen}} = 0.5$ monolayers (ML; 1 ML is defined as the number of surface atoms on the unreconstructed Pt(1 1 0) surface) into a (3×1) phase, which we interpret as a CDW phase [15, 32]. Finally, inverse photoemission results revealed the existence of an unoccupied 1D surface state on Pt(1 1 0), located on the close-packed atom chains [33]. All these observations prompted us to look for low-dimensional electronic states and possible correlation effects on the Pt(1 1 0) surface.

2. Experimental setup

The measurements were carried out in a UHV apparatus with a base pressure of 7×10^{-11} mbar. The Pt(1 1 0) single crystal was cut and polished to a precision of $\pm 0.1^\circ$. It was mounted on a

five-axis manipulator with electron bombardment heating and $N_{2\text{liq}}$ cooling facilities. The light source was a SPECS UVS 300 high-pressure plasma lamp. For some spectra, the light was filtered by a SPECS TMM 302 toroidal mirror monochromator, eliminating satellite photon lines and yielding $>90\%$ linearly polarized light. Spectra were recorded by an OMICRON AR 65 concentric hemispherical analyser mounted on a two-axis goniometer. For recording photoemission intensities along k directions, which do not intersect the $\bar{\Gamma}$ point, both the polar and the azimuthal angle are varied. The angular resolution of the analyser is $\pm 0.65^\circ$ and the energy resolution can be varied from 10 meV upward. The spectra presented here were recorded with $\Delta E = 65$ meV. Additionally, spectra with variable photon energy were recorded at the VUV beamline of the ELETTRA electron storage ring with an overall resolution of 45 meV.

The sample was initially cleaned by standard procedures until a good (1×2) missing-row reconstruction was observed in low-energy electron diffraction (LEED). Prior to each ARUPS measurement, traces of residual carbon were eliminated by two cycles of oxygen adsorption at $T < 140$ K and subsequent flash desorption. Only when no trace of CO_2 could be detected in the thermal desorption spectrum, the sample was judged to be clean. Bromine was dosed directly onto the sample from a solid-state electrolysis cell [15]. LEED investigations were carried out by recording the images with a highly sensitive CCD camera and subsequent intensity $I(V)$ and spot profile analysis $I(T)$ of the stored images.

3. Results and discussion

Figure 2 shows the structure of (i) the $\text{Pt}(1\ 1\ 0)$ - (1×2) missing-row reconstructed surface [34], (ii) the $c(2 \times 2)$ -Br/ $\text{Pt}(1\ 1\ 0)$ surface [34] and (iii) the (3×1) -Br/ $\text{Pt}(1\ 1\ 0)$ surface [32]. For each of these surfaces, the first-to-second layer distance d_{12} obtained from $I(V)$ -LEED and DFT calculations is also given in figure 2. In addition we investigated the H/ $\text{Pt}(1\ 1\ 0)$ surface with an H coverage of $\Theta_{\text{H}} = 0.5$ ML. The surface structure is the same as that of the clean $\text{Pt}(1\ 1\ 0)$ - (1×2) surface, but with each short-bridge site being decorated by H [35]. For H/ $\text{Pt}(1\ 1\ 0)$, d_{12} is given in figure 2(a) in parentheses. In figures 2(d)–(f) the corresponding SBZs are outlined.

Figure 3 shows greyscale images of the photoelectron intensity distributions for the three different surface structures of figure 2 as a function of binding energy and k vector along the line $\bar{Y}\bar{S}$ (H adsorption changes the intensity, but not the dispersion of the clean surface features). An intense QP feature right at E_{F} with the same dispersion around \bar{S} is found in all cases. On the (3×1) surface, the band is folded back at the new SBZ boundaries as expected, but the back-folded band is seen with surprisingly similar intensity throughout the new SBZs. If the back-folding would be due to a final state umklapp, one should expect strong intensity differences between the primary cone emission and the back-folded bands. Hence, we conclude that the threefold periodicity is due to an initial-state effect, a remapping of the band in the new SBZ by the additional Fourier component of the potential in the (3×1) -Br/ $\text{Pt}(1\ 1\ 0)$ system. This component is confined to the surface. Therefore, the intense back-folding reveals the surface character of the band (strictly speaking, it is a surface resonance, because there is no projected bulk band gap in that energy region).² Additionally, the QP peak at \bar{S} was investigated with different photon energies. As shown in figure 4, no k_{\perp} dispersion was observed, corroborating the assignment to a surface feature.

² Analysis of the LEED-IV data suggests that the main contribution to the (3×1) -Fourier component is actually due to the buckling in the topmost Pt layer rather than the Br itself.

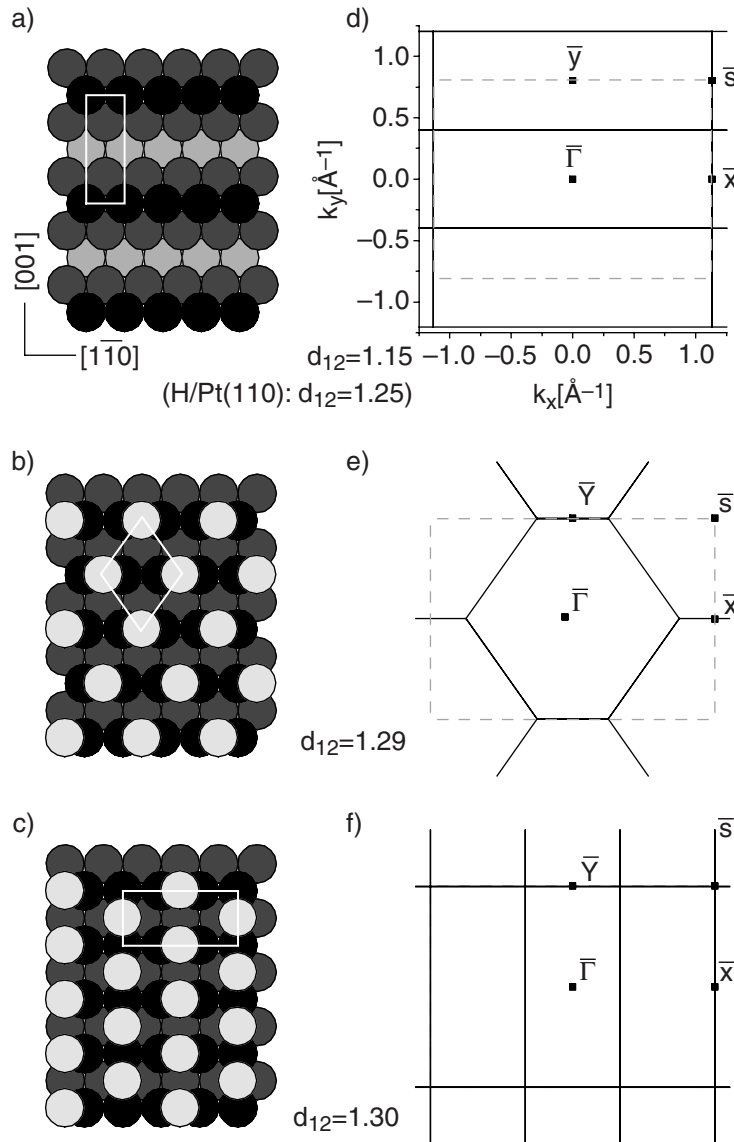


Figure 2. (a) Real-space structure of the clean Pt(110)-(1 × 2) missing row reconstructed surface, (b) of the $c(2 \times 2)$ -Br/Pt(110) surface and (c) of the (3×1) -Br/Pt(110) surface. Top layer Pt atoms are depicted in black; Br atoms are light-grey. The structure of the H/Pt(110) system discussed in the text is the same as the Pt(110)-(1 × 2) structure, but with every short-bridge site occupied by a H atom. The first-to-second layer distance d_{12} is also given for all surfaces. (d, e, f) The SBZs for the surfaces shown in (a, b, c). The high symmetry points \bar{X} , \bar{Y} and \bar{S} refer to the (1×1) SBZ (dashed lines).

Given that the QP peak at \bar{S} is due to a surface resonance, figure 3 contains additional information: firstly, the Br adlayer does not shift the band, nor is the band width significantly influenced. Apparently, the interaction of the Br orbitals with this band is very weak. Even more significant, the band is not influenced in width and position by the lifting of the (1×2) reconstruction. We conclude that there is almost no interaction from row to row even when the

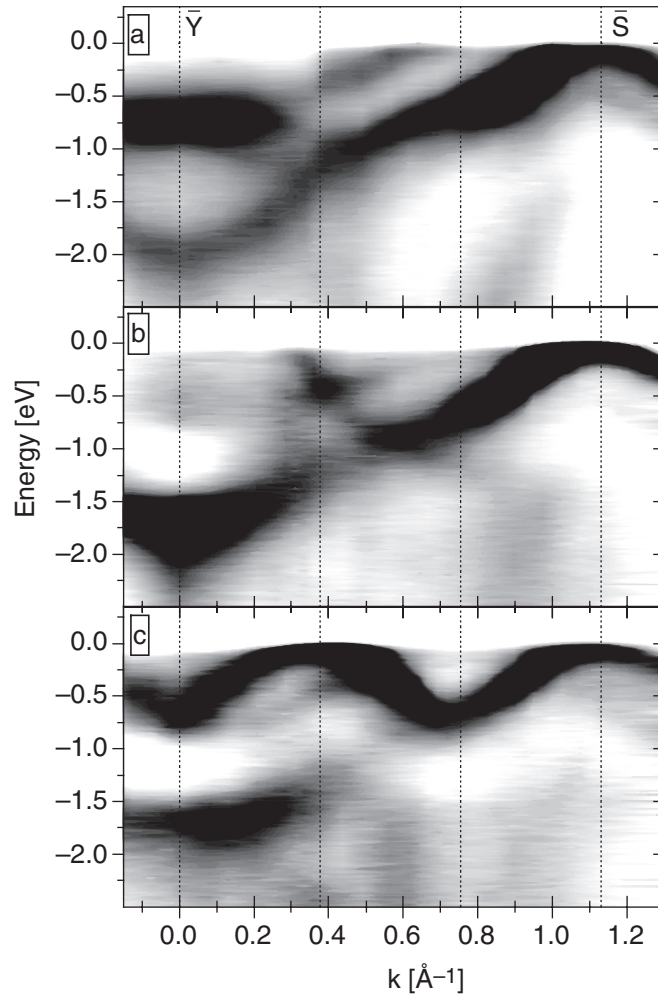


Figure 3. Photoemission intensity distribution along the line $\bar{\Gamma}\bar{S}$ for the clean Pt(1 1 0)-(1 \times 2) surface (a), the c(2 \times 2)-Br/Pt(1 1 0) surface (b) and the (3 \times 1)-Br/Pt(1 1 0) surface (c). High intensities are shown in black, and low intensities in white. Energies are referenced to E_F . All spectra have been recorded with monochromatic light ($h\nu = 21.22$ eV). In order to sample the k space the analyser is moved, while the angle of incidence of the photons is kept constant. The polarization vector is strictly parallel to the close-packed rows.

distance between adjacent rows is reduced to 3.92 \AA . Consequently, the surface resonance band has a quasi-1D character.

If the \bar{S} QP peak at the Fermi level is due to a surface resonance, it should not only sample the (3 \times 1) Fourier component of the surface potential in the (3 \times 1)-Br/Pt(1 1 0) structure, but also the (1 \times 2) Fourier component in the missing row structure. In other words, on the clean Pt(1 1 0) surface the QP peak should appear also at \bar{X} . This is indeed the case, as illustrated in figure 5(a) which shows the photoelectron intensity distribution along $\bar{X}\bar{S}$. The QP peak is seen at \bar{S} and \bar{X} , while in between the band disperses above the Fermi level. In order to assess the total band dispersion in the k_y direction, i.e. perpendicular to the close-packed rows, we measured the dispersion also at $k_x = 1.29$ \AA^{-1} (see figure 5(b)). Here, the whole band falls below E_F and a total

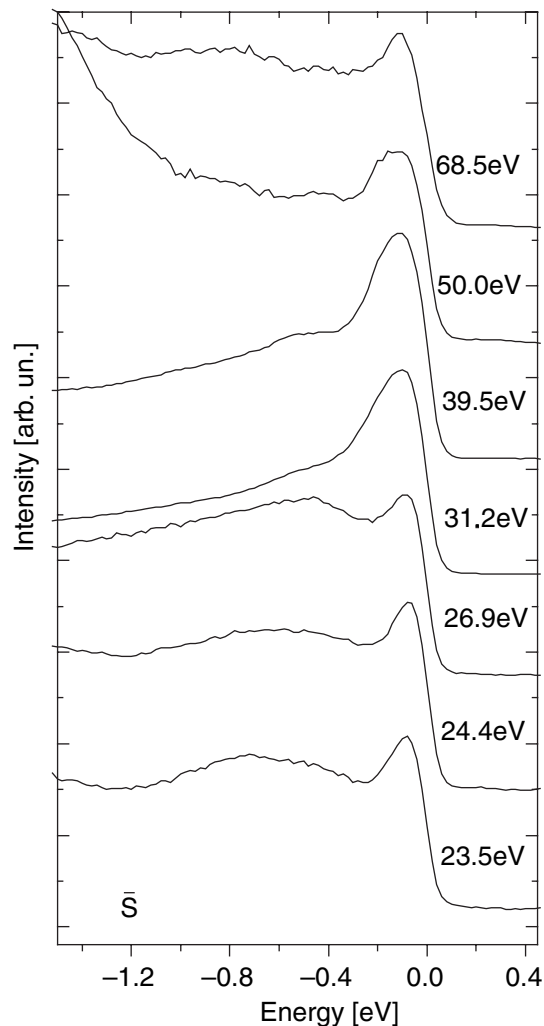


Figure 4. Energy distribution curves, recorded in such a way that $k_{||}$ around E_F coincides with the \bar{S} point, as a function of photon energy.

dispersion of <200 meV is revealed. In summary, we observe for all investigated surface systems, a surface resonance band around \bar{S} with a hole-like dispersion around \bar{S} in the $\bar{Y}\bar{S}$ direction and a weak electron-like dispersion in the $\bar{X}\bar{S}$ direction. Thus at \bar{S} we have a saddle point at the Fermi level, which is associated with an intense QP feature. The temperature-dependent behaviour of this QP feature on the $c(2 \times 2)$ -Br/Pt(1 1 0) surface has been reported previously [36], but we briefly review the results here in connection with new data on the $c(2 \times 2) \rightarrow (1 \times 1)$ order-disorder transition.

Figure 6(a) shows the reduction of the \bar{S} QP peak intensity as a function of temperature. Curiously, the temperature range in which we observe the peak height reduction is centred about a critical temperature, where an order-disorder phase transition takes place. Figures 6(b)–(d) show the behaviour of the $(1/2, 1/2)$ LEED spot of the $c(2 \times 2)$ structure as a function of temperature. The spot profile in $[001]$ direction, i.e. perpendicular to the close-packed rows, is fitted by a sum of a Gaussian and a Lorentzian [37]. A breakdown of the Gauss height with an onset at ~ 360 K indicates a phase transition. The height of the Lorentzian component (figure 6(c)) rises at the same

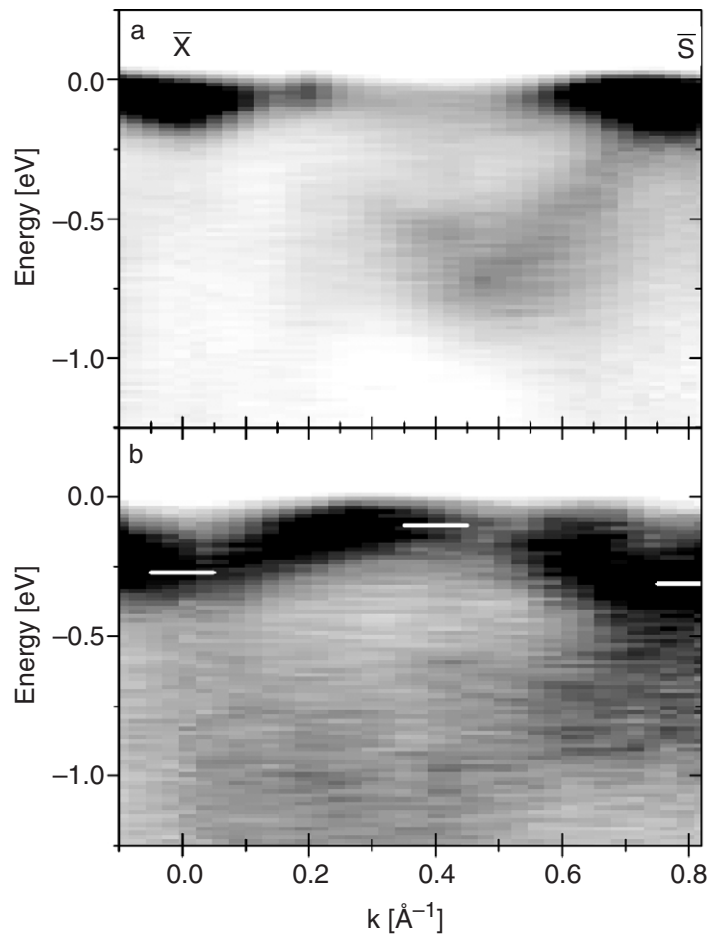


Figure 5. Photoemission intensity distribution along the line $\bar{X}\bar{S}$ (a) and along the line ($k_x = 1.29 \text{ \AA}^{-1}, 0 \leq k_y \leq 0.8 \text{ \AA}^{-1}$) for the clean Pt(1 1 0)-(1 \times 2) surface. The lines in (b) mark the minimum and maximum, respectively, of the band dispersion.

temperature dramatically and signals a divergence in the susceptibility of the order parameter. Of course, the divergence itself is not observable, but is rounded off due to finite instrumental resolution [38] and finite domain size [39]. Finally, the correlation length, which is inversely proportional to the Lorentzian width, is also seen to increase enormously at 360 K (figure 6(d)). All these changes are characteristic for a second-order phase transition from the $c(2 \times 2)$ into a disordered (1×1) structure. The integral spot profiles do not change in this temperature range apart from the monotonic decrease according to the usual Debye–Waller behaviour. Also, the half-order spot profile in $[1 \bar{1} 0]$ direction, i.e. along the rows, remains almost unchanged apart from a slight continuous intensity decrease above ~ 400 K. The latter observations indicate first that the substrate is not involved in the phase transition and second that the order along the rows is not destroyed. Hence the Br–Br distance along the rows remains unchanged and the order–disorder transition results from a loss of a defined phase relation between the rows. The disordered (1×1) structure can then be visualized as an array, where the phase difference of Br sequences on neighbouring rows alternates randomly between 0 and π . This is in agreement with STM observations [15] and DFT calculations [40], which both show that the two structures are very close in energy.

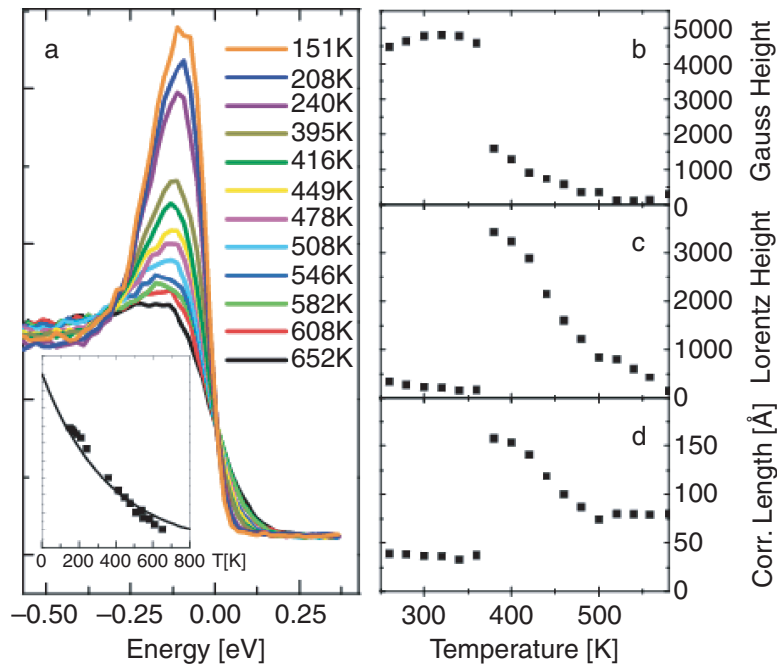


Figure 6. (a) Intensity change of the QP peak at \bar{S} as a function of temperature for the $c(2 \times 2)$ -Br/Pt(1 1 0) surface. (b)–(d) Spot profile analysis of the $(1/2, 1/2)$ LEED spot for the $c(2 \times 2)$ -Br/Pt(1 1 0) surface: decrease of the Gaussian peak height (b), evolution of the Lorentz peak height (c) and evolution of the correlation length (inverse Lorentz line width) (d).

The QP peak height is reduced by about 50% just at the critical temperature for the $c(2 \times 2) \rightarrow (1 \times 1)$ order–disorder transition. Yet the temperature dependence of the QP peak height shows no anomaly whatsoever at the critical temperature. Rather the decrease of the QP peak height is almost linear. The inset in figure 6(a) compares the measured data (points) with a Debye–Waller function obtained by assuming a momentum transfer of 2.26 \AA^{-1} corresponding to a reciprocal lattice vector. Such a fit yields an apparent Debye temperature Θ_D of 35 K in stark contrast to the surface Debye temperature of 107 K for clean Pt(1 1 0) [41]. On fcc surfaces a strong anisotropy of the vibrational modes can be expected. However, a typical value for this anisotropy is of the order of 3 : 2 for the effective Debye temperature along and perpendicular to the close-packed rows, respectively [42]. Therefore, the anisotropy cannot account for such a difference as found here. The absence of a critical behaviour indicates that the QP peak is not sensitive to long-range order in the Br layer and hence is not influenced by the fluctuations at the phase transition. This is somewhat unexpected, but we have already seen that the surface resonance is remarkably stable with respect to changes in the Br coverage. The extremely low apparent Debye temperature Θ_D obtained from the ARUPS intensity could in principle originate in a soft mode of the Br layer. However, from an evaluation of the $c(2 \times 2)$ -LEED integral-order spots, we obtained $\Theta_D \approx 110 \text{ K}$ and examination of the half-order spots below 360 K yields a similar result. Thus the anomalously strong temperature dependence of the \bar{S} QP peak does not seem to be correlated with the Br overlayer. In fact, we find an apparent Θ_D as low as 40 K also for a QP peak at \bar{X} on the H/Pt(1 1 0)-(1 \times 2) surface as discussed below. Matzdorf *et al* [43]

were able to explain an exceptionally strong temperature dependence of ARUPS bulk transitions by the interference of multiple scattered waves in the final state. Such an explanation seems very unlikely in the present case, because we observe the anomalous temperature dependence with the same photon energy at different points in k space and hence different k_{\perp} as well as k_{\parallel} . For Shockley surface states on fcc(1 1 1) surfaces, Goldmann and coworkers also observed a strong T dependence [44], which was also in conflict with the standard Debye–Waller model. However in this case, the reduction of the QP peak height was associated with a significant broadening of the peaks in contrast to the present Tamm-state QP peak. We therefore look for a different mechanism that raises the temperature sensitivity of ARUPS peaks far beyond the predictions from a simple Debye–Waller scheme. A possible mechanism hinges on the weak dispersion of the surface resonance band perpendicular to the rows. We start from the ideal periodic crystal at $T = 0$ K. Here, the periodic lattice potential couples only wave functions, whose wave vector differs by a reciprocal lattice vector. Increasing the temperature introduces a weak random perturbing potential with a broad spectrum of Fourier components, which can couple wave functions with almost arbitrary wave vector difference. For a strongly dispersing band, however, the coupling is only resonant in the immediate neighbourhood of a given k vector. For wave functions with larger k vector differences, the coupling is strongly non-resonant and therefore negligible. For a very weakly dispersing band, in contrast, a near-resonant coupling is possible throughout the SBZ. Thus, even weak perturbing potentials are able to mix a broad spectrum of k vectors into a given wave function. As a consequence, localized wave packages are obtained and the phase coherence between different locations in real space is lost. ARUPS from a localized initial state, however, results in a strong many-body response. Therefore, ARUPS intensity is transferred from well-defined QP peaks to the incoherent background. Within this model, the band dispersion determines the response of the wave functions to thermal excitation. Weak dispersion results in a rapid temperature-induced decoherence and consequently a quenching of the QP peak.

The temperature dependence of the QP peak is very similar to what has been observed in other systems, where coherent–incoherent transitions take place, for instance at a Mott transition [5] or in Kondo systems [20]. It is therefore interesting to compare the present model to the Anderson impurity model (AIM), which is usually adopted as a starting point for discussions of the Kondo or Mott–Hubbard systems. In the AIM, the ground state is a hybrid state formed from a linear combination of the impurity level and conduction band states. In the present system, the impurity levels are associated with the quasi-1D chain states localized on individual close-packed rows (rendering the system in a sense, a 1D analogue of a Kondo lattice). These chain states have no direct overlap due to the comparatively large separation between the rows. They do, however, weakly interact with the 3D manifold of the bulk d band continuum. Thus there is a residual-through-substrate interaction which is the analogue of the hybridization matrix element V in the AIM. Emission from this extended, coherent ground state gives rise to the QP peak at \bar{S} . An increase in T results in a perturbing potential as discussed above. The perturbation gives rise to an Anderson-type localization which splits-off the localized states from the ground state [16, 17], much as a gradual increase in the Hubbard U splits localized states off an extended conduction band [45]. In the present case, the energy difference between the extended ground state and the split-off localized states is essentially the kinetic energy associated with the localization on individual chains and therefore proportional to V^2 . Thus V^2 sets the temperature scale for the coherent–incoherent transition. In the photoemission spectra, the increasing localization with rising temperature manifests itself as a spectral weight transfer from the coherent QP peak to incoherent emission from the ensemble of localized chain states.

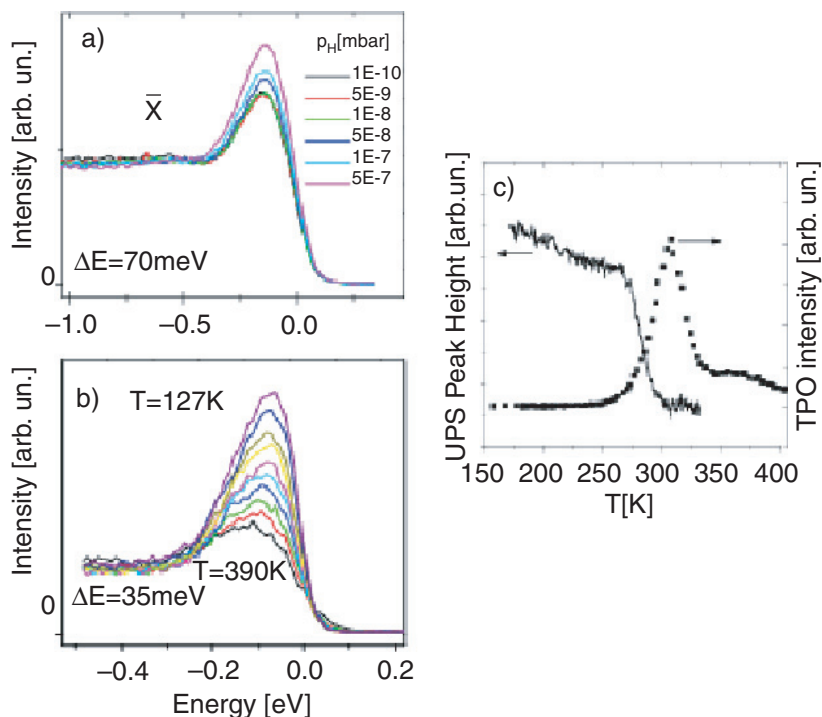


Figure 7. Change of the QP peak at \bar{X} on Pt(1 1 0)-(1 \times 2) as a function of H₂ equilibrium pressure at 320 K (a); change of the QP peak at \bar{X} as H adsorbs during cooling from 390 to 127 K in an H₂ background pressure of $\sim 4 \times 10^{-10}$ mbar (b); decrease of the QP peak height and H₂ temperature programmed desorption spectrum (dots) recorded after adsorption of 0.5 ML H at 127 K (c). Here, the photoemission spectra were recorded with unpolarized light ($h\nu = 21.22$ eV).

We now turn to a discussion of the \bar{X} QP peak intensity on the Pt(1 1 0)-(1 \times 2) surface. The intensity of this feature depends strongly on the presence of H on the surface. This is illustrated in figure 7(a), which shows a pronounced increase of the peak height as the H equilibrium coverage is increased at a fixed temperature of 320 K. Figure 7(b) shows the results of a complementary experiment: the Pt(1 1 0)-(1 \times 2) surface was cooled down from 390 to 127 K at a H₂ background pressure of $\sim 4 \times 10^{-10}$ mbar, so as to obtain a coverage of 0.5 ML. At this coverage, every short-bridge site on the topmost close-packed rows is occupied [35]. This H adsorption structure is correlated with the so-called β_2 -desorption peak of H₂ [46, 47]. With the β_2 H state initially saturated, the surface was now gradually heated to 390 K while recording EDCs. Qualitatively, the changes in the \bar{X} QP peak resemble very much the changes reported for the \bar{S} QP peak in figure 6(a). In figure 7(c), the reduction of the peak intensity is related to the desorption peak of H₂. A strong temperature dependence is observed even before the on-set of H₂ desorption. From the QP peak height decay at $160 \text{ K} < T < 260 \text{ K}$, one would obtain an apparent Θ_D of ~ 40 K, similar to the one observed for the \bar{S} QP peak in the $c(2 \times 2)$ -Br/Pt(1 1 0) structure. However, in addition to this monotonic T dependence, a dramatic loss of intensity is associated with desorption of H from the β_2 state. The \bar{X} QP peak is large when the β_2 state is fully populated and nearly quenched for the clean Pt(1 1 0) surface.

The most simple explanation at hand is a H-induced peak shift. H is generally known to pull down surface states in energy due to the attractive potential of the proton [48]–[50]. Thus,

if the \bar{X} feature peaked above the Fermi level on the clean surface and was pulled below E_F by adsorbed H, one should expect a QP peak to grow at E_F . However, this possibility can be excluded, because the surface resonance at \bar{X} is located below E_F already on the clean surface. The band is completely occupied throughout the SBZ, including the \bar{S} and the \bar{X} points (figure 5(a)), with the exception of a small hole pocket midway between the \bar{X} and the \bar{S} points. The size of this pocket as determined from an ARUPS scan similar to the one shown in figure 5(a) is independent of the H coverage within our measurement accuracy for $0 \leq \Theta_H \leq 0.5$ ML. The absence of an energetic interaction with H is consistent with the band dispersion: at \bar{X} it reaches a local maximum as a function of k_x , hence the associated wave function is anti-bonding along the $[1 \bar{1} 0]$ direction. This implies the existence of nodal planes halfway between the close-packed atoms, i.e. at the H adsorption sites. We therefore look for a different explanation of the H-induced intensity change of the \bar{X} QP peak.

As mentioned above, the QP peak at \bar{X} originates in the same surface band as the QP peak at \bar{S} . Due to the additional Fourier component in the surface potential, which stems from the (1×2) reconstruction, the surface resonance contains a linear combination of wave functions with wave vectors $k_{\bar{S}} = (1.13, 0.8) \text{ \AA}^{-1}$ and $k_{\bar{X}} = (1.13, 0.0) \text{ \AA}^{-1}$. Therefore, emission is observed in both, the \bar{S} and the \bar{X} direction. Now it is conceivable that H changes the strength of the relevant Fourier component in the surface potential thereby enhancing the $k_{\bar{X}}$ admixture and consequently the QP peak intensity at \bar{X} (one could call this an initial-state umklapp). There are problems with this explanation too. First of all, H is a weak scatterer in comparison to Pt. It is rather unexpected that the decoration of the Pt rows with H (note that the (1×2) reconstruction remains unchanged) should enhance the Fourier component to such an extent that the QP peak intensity increases by a factor of three or more. It is true that the H adsorption causes also a partial removal of the inward relaxation of the topmost Pt rows, but again this is a small change.

Another observation is relevant in this context: figure 7(c) shows that the \bar{X} QP peak-height reduction is essentially associated with a H coverage change from 50% of a ML to about 20% of an ML, which takes place upon warming up to ~ 300 K. The remaining 0.2 ML H causes little change of the peak height. Note that at this temperature, the weakly attractive H–H interaction at the surface [35] is overcome by thermal excitation and H is distributed as a mobile 2D gas on the surface. On the other hand, we observed during H uptake measurements at $T < 150$ K that the peak height scaled linearly with the H uptake from the very beginning, in apparent contrast to figure 7(c) which seems to imply that up to 0.2 ML of H are irrelevant for the peak intensity. The apparent contradiction is resolved, if one realizes that at low temperatures due to the attractive interaction the H agglomerates in islands on the (1×2) surface. Thus we conclude that an ordered arrangement of H in islands, where every short-bridge site is occupied, is essential for the observed changes in the \bar{X} QP peak. A disordered H gas mobile along the rows would not yield this effect. In contrast, neither the directly H-induced Fourier component nor the one stemming from the relaxation of the rows should strongly depend on whether the H is mobile or not.

A third consideration concerns the redistribution of photoemission intensity. If the intensity of the QP peak is governed by the strength of an initial-state umklapp, one should expect an elastic intensity transfer from \bar{S} to \bar{X} and vice versa. This is not observed. Rather, the \bar{X} QP peak seems to exchange intensity with an ill-defined feature close to \bar{S} , but at higher binding energy. This is illustrated in figures 8(a) and (b), showing photoemission intensity distribution curves measured along $\bar{X} \bar{S}$ as a function of binding energy for the clean (figure 8(a)) and the H covered surface (figure 8(b)). The higher-binding-energy feature at \bar{S} is rather delocalized in k

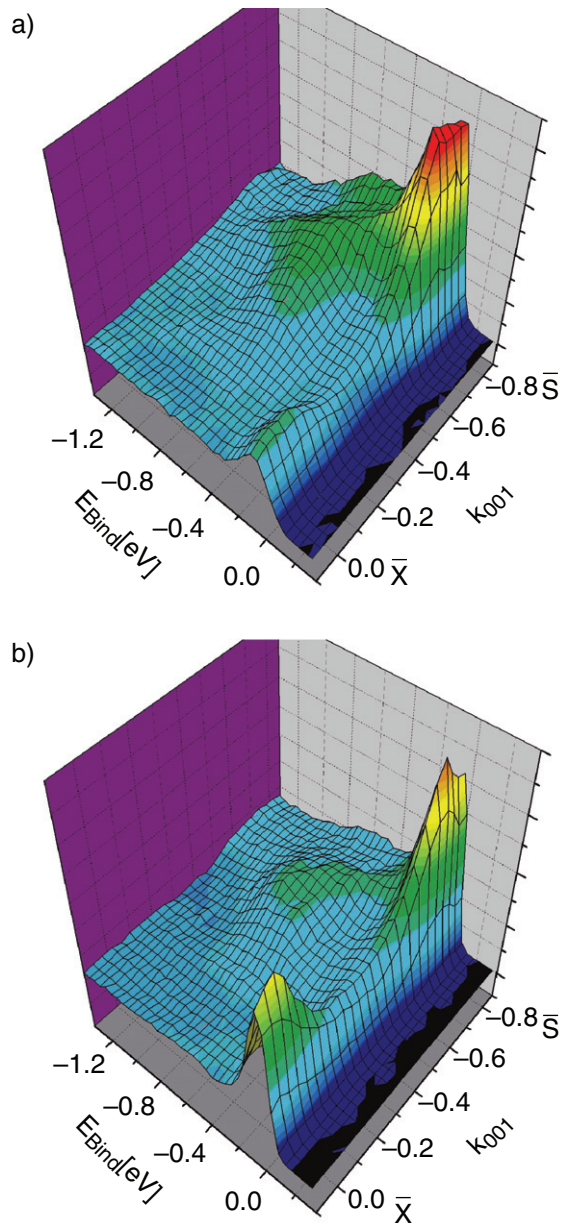


Figure 8. Photoemission intensity distribution between the \bar{X} and the \bar{S} point for the clean Pt(1 1 0)-(1 \times 2) surface (a) and the Pt(1 1 0)-(1 \times 2) surface covered with 0.5 ML H. Note the intensity transfer from the diffuse feature around \bar{S} at a binding energy of 0.8–1.2 eV in (a) to the QP peak at \bar{X} in (b). Light polarized parallel to the close-packed rows ($h\nu = 21.22$ eV).

space, which hints towards emission from a more localized initial state as compared to the QP features seen at \bar{X} and \bar{S} . In order to account for the H-induced QP intensity change at \bar{X} , we again propose a coherent–incoherent transition as outlined in more detail below.

As we have seen, the surface resonance band at \bar{S} and \bar{X} disperses strongly along k_x but the dispersion from \bar{X} to \bar{S} amounts to <200 meV. Thus the band is strongly anisotropic and may be termed quasi-1D. 200 meV is still a sizeable dispersion, but thermal energies at room temperature

are no longer negligible in comparison to the bandwidth. As discussed above, any perturbing potential of that order of magnitude might in fact result in at least partial localization of the wave-function along individual close-packed rows. Such an Anderson-type localization would then cause a transition from a 2D surface resonance composed of an ensemble of phase-coherently coupled chain states to a collection of incoherent 1D chain states. The stronger localization in the latter case causes a stronger many-body response with the effect of a much wider energy and momentum distribution of the resulting ARUPS final states. In two previous studies [18, 27], we have described such a transition for the *s,p* derived Shockley surface state on the striped O/Cu(1 1 0) surface. The characteristic features reported there have much in common with the present data: a disappearance of QP peaks at high symmetry points of the SBZ and a redistribution of intensity into less well-defined features with different angular distribution. If the changes of the \bar{X} QP peak intensity are due to a coherent–incoherent transition, then one has to conclude that the H β_2 state favours the formation of a coherent 2D surface resonance, or in other words increases the coupling between the 1D Tamm states. The following scenario could be envisioned: on the clean surface, the (1×2) reconstruction creates a very open surface with the outermost atoms experiencing an entirely different environment as in the bulk. To restore the optimal electron density at least partially, the surface atom rows undergo a strong inward relaxation resulting in a structure which deviates significantly from the bulk. In this specific environment, a 1D Tamm state is split-off and shifted upwards from the topmost occupied *d* band. As the surface is covered with H, a more bulk-like environment is established for the topmost atom rows and the geometry relaxes partially back towards the bulk-truncated structure [35]. The splitting between the Tamm state and the parent bulk *d* band is reduced, giving rise to a slightly improved coupling between them. The increased coupling to the bulk is responsible for a through-substrate coupling of the 1D Tamm states, establishing a phase coherence and the formation of a 2D surface resonance. Note that the energy shifts implied by this scenario are very small, because minute changes of the coupling strength are sufficient to tilt the balance in favour of coherent or incoherent behaviour, respectively. In summary, while we are not able to completely rule out a H-induced change of the (1×2) Fourier component of the surface potential to be responsible for the observed H induced changes of the \bar{X} QP particle peak intensity, we propose an explanation in terms of a coherent–incoherent transition. The spectral changes display a striking similarity with a vast number of other systems, where such coherent–incoherent transitions take place [21, 51, 52]–[54] and circumstantial evidence is strongly in favour of the latter interpretation.

The QP peak at \bar{X} observed in the H/Pt(1 1 0)- (1×2) system is almost quenched at room temperature on clean Pt(1 1 0)- (1×2) . Consequently, the coherence is already lost at $T = 300$ K. In contrast, the QP peak observed for the $c(2 \times 2)$ structure at \bar{S} is quenched only for temperatures above 500 K, thus appearing much more stable. This is consistent with the lifting of the missing-row reconstruction upon Br adsorption. In the $c(2 \times 2)$ structure, the rows are more closely spaced, hence the interaction from row to row is increased and the (partial) coherence preserved up to a higher temperature.

Accepting the presence of quasi-1D surface states on Pt(1 1 0) and the occurrence of coherent–incoherent transitions we may ask ourselves, whether there is additional evidence for correlation effects. Of course our previous report of a CDW-induced phase transition on the halogenated Pt(1 1 0) surface fits well into this pattern [15, 32]. But one should also expect direct fingerprints of correlation to turn up in the ARUPS spectra. In figure 9 we show close-ups of the dispersion of the \bar{S} surface resonance. In all three cases, a kink appears in the dispersion as the surface band approaches E_F , accompanied by a considerable mass renormalization. The

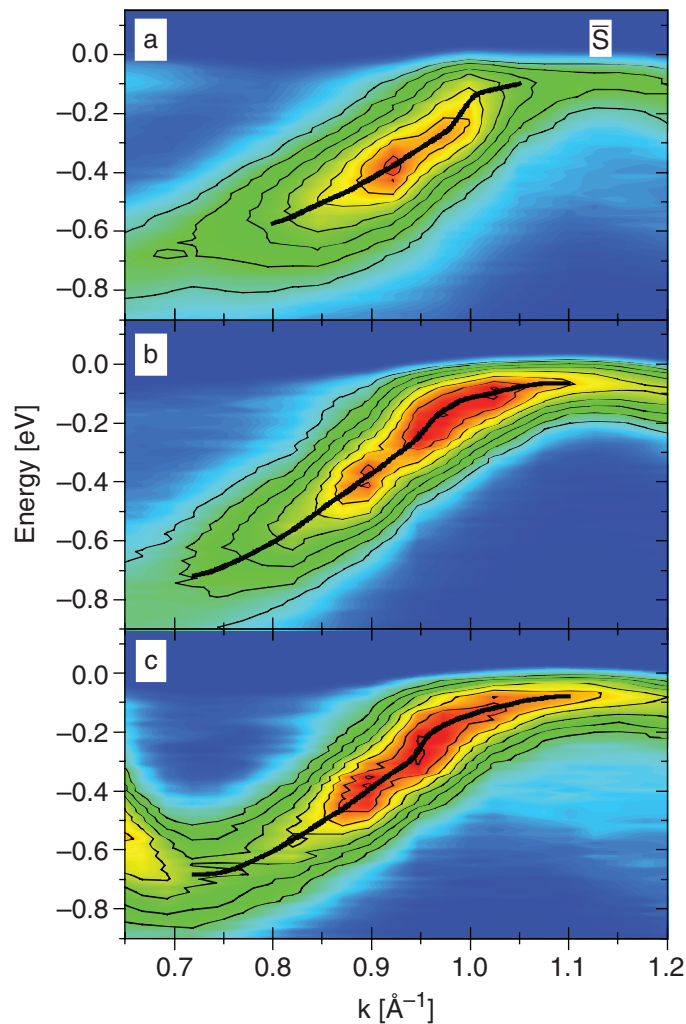


Figure 9. Contour plot of the photoemission intensity distribution close to the \bar{S} point along the line $\bar{\Gamma}\bar{S}$ showing details of the dispersion for the clean Pt(1 1 0)-(1 \times 2) surface (a), the c(2 \times 2)-Br/Pt(1 1 0) surface (b) and the (3 \times 1)-Br/Pt(1 1 0) surface (c). Lines along the maximum of the intensity distribution are drawn to guide the eye. The kinks occur all around 300 meV. Light polarized parallel to the close-packed rows ($h\nu = 21.22$ eV).

deviation from the smooth, continuous dispersion occurs at ~ 300 meV (see lines in figure 9). Such kinks are characteristic for the interaction of the QPs with a bosonic excitation [55]. From an evaluation of this anomaly, one can derive the real part of the self-energy which in turn yields the electron–boson coupling [56, 57]. In the present examples, the energy scale set by the point of deviation is too large for phonons. Possible alternatives include spin excitations and charge oscillations in a quasi-1D electron gas (holons). At this stage it is too early to speculate about the nature of the mode involved, although we mention recent calculations by Delin and Tosatti [58, 59] proving that isolated chains of close-packed Pt atoms are indeed ferromagnetically ordered.

On first sight it might appear unlikely that a coupling to bosonic excitations which are sufficiently strong to explain the observed kinks should occur in a band, which is almost completely occupied. Particularly, on the clean Pt(1 1 0)-(1 × 2) surface, there is only a tiny hole pocket between \bar{S} and \bar{X} providing little phase space for the virtual excitations. For that reason we assume that interband excitations are involved. Unfortunately, scalar-relativistic DFT slab calculations, so far, failed to produce any of the observed surface resonances [60]. Spin-orbit coupling is certainly essential for a detailed description of the electronic band structure and for magnetic ordering effects in Pt [58], but DFT band structure calculations will also fail to correctly describe correlation effects in low-dimensional electronic states.

In conclusion, we presented ARUPS data for clean and adsorbate covered Pt(1 1 0) showing a quasi-1D surface resonance. The surface resonance produces a sharp QP peak at the Fermi level, which shows anomalous changes of intensity as a function of temperature and adsorbate coverage. The changes are consistently interpreted as coherent–incoherent transitions. The 1D character of the surface resonance is expected to lead to considerable electronic correlation effects. Indeed we observe kinks in the surface band dispersion and a strong mass renormalization close to E_F . Thus, the Pt(1 1 0) surface appears to be a correlated system well suited for a model study. Further progress in the elucidation of the correlation effects will require a systematic examination of the photon energy dependence of the spectral features and of possible magnetic ordering effects.

Acknowledgments

We thank A Goldmann for a critical reading of the manuscript. We gratefully acknowledge technical support at ELETTRA by C Crotti (ISM, Italy) and financial support by the Austrian Science Fund through projects P-14988 and S9001-N04.

References

- [1] Bishop A R 1997 *Synth. Met.* **86** 2203
- [2] Adapted from Bourbonnais C 2000 *J. Phys. IV France* **10** Pr3-81
- [3] 2001 *J. Electron Spectrosc. Relat. Phenom.* **117–118**
- [4] Kordyuk A A *et al* 2002 *Phys. Rev. Lett.* **89** 077003–1
- [5] Mo S-K *et al* 2003 *Phys. Rev. Lett.* **90** 186403
- [6] Hwang J, Timusk T and Gu G D 2004 *Nature* **427** 714–17
Cuk T, Shen Z-X, Gromko A D, Sun Z and Dessau D S 2004 *Nature* **432**
Hwang J, Timusk T and Gu G D 2004 *Nature* **432**
- [7] Melechko A V, Braun J, Weitering H H and Plummer E W 1999 *Phys. Rev. Lett.* **83** 999
- [8] Voit J 2001 *J. Electron Spectrosc. Relat. Phenom.* **117–118** 469
- [9] Kim C, Shen Z-X, Motoyama N, Eisaki H, Uchida S, Tohyama T and Maekawa S 1997 *Phys. Rev. B* **56** 15589
- [10] Segovia P, Purdie D, Hengsberger M and Baer Y 1999 *Nature* **402** 504
- [11] Losio R, Altmann K N, Kirakosian A, Lin J-L, Petrovykh D Y and Himpsel F J 2001 *Phys. Rev. Lett.* **86** 4632
- [12] Grioni M, Perfetti L and Berger H 2004 *J. Electron Spectrosc. Relat. Phenom.* **137–140** 417–23
- [13] Tosatti E 1995 *Electronic Surface and Interface States on Metallic Systems* ed E Bertel and M Donath (Singapore: World Scientific) p 67
- [14] Aruga T 2002 *J. Phys.: Condens. Matter* **14** 8393
- [15] Swamy K, Menzel A, Beer R and Bertel E 2001 *Phys. Rev. Lett.* **86** 1299
- [16] Ziman J M 1969 *J. Phys. C: Solid State Phys.* **2** 1230
- [17] Koslowski Th, Rowan D G and Logan D E 1996 *Ber. Bunsenges. Phys. Chem.* **100** 101

- [18] Berge K, Gerlach A, Meister G, Goldmann A and Bertel E 2004 *Phys. Rev. B* **70** 155303
- [19] Fulde P 1991 *Electron Correlations in Molecules and Solids* (Berlin: Springer) p 310
- [20] Malterre D, Grioni M and Baer Y 1996 *Adv. Phys.* **45** 299
- [21] Valla T *et al* 2002 *Nature* **417** 627
- [22] Feng D L *et al* 2000 *Science* **289** 277
- [23] Tranquada J M *et al* 2004 *Nature* **429** 534
- [24] Carlson E W, Orgad D, Kivelson S A and Emery V J 2000 *Phys. Rev. B* **62** 3422
- [25] Kevan S D (ed) 1992 *Angle-Resolved Photoemission (Studies in Surface Science and Catalysis vol 74)* (Amsterdam: Elsevier)
- [26] Kern K *et al* 1991 *Phys. Rev. Lett.* **67** 855
- [27] Bertel E and Lehmann J 1998 *Phys. Rev. Lett.* **80** 1497
- [28] Kagoshima S, Nagasawa H and Sambongi T 1982 *One-dimensional conductors (Solid State Sciences vol 72)* (Berlin: Springer)
- [29] Fay D and Appel J 2002 *Phys. Rev. Lett.* **89** 127001
- [30] Herrmannsdörfer T, Rehmann S, Wendler W and Pobell F 1996 *J. Low Temp. Phys.* **104** 49
- [31] Chang C S, Su W B, Wei C M and Tsong T T 1999 *Phys. Rev. Lett.* **83** 2604
- [32] Deisl C *et al* 2004 *Phys. Rev. B* **69** 195405
- [33] Memmel N, Rangelov G and Bertel E 2003 *Prog. Surf. Sci.* **74** 239
- [34] Blum V *et al* 2002 *Phys. Rev. B* **65** 1654081
- [35] Zhang Z *et al* 2004 *Phys. Rev. B* **70** 121401
- [36] Menzel A, Beer R and Bertel E 2002 *Phys. Rev. Lett.* **89** 076803
- [37] Pfnür H, Voges C, Budde K and Schwenger L 1996 *Prog. Surf. Sci.* **53** 205
- [38] Roelofs L D 1982 *Appl. Surf. Sci.* **11/12** 425
- [39] Michailov M, de Beauvais C, Rouxel D and Mutaftschiev B 2000 *Phys. Rev. B* **61** 5987
- [40] Franchini C 2002 *PhD Thesis* Vienna University of Technology
- [41] Van Hove M A, Weinberg W H and Chan C-M 1986 *Low-Energy Electron Diffraction (Springer Series in Surface Science vol 6)* (Berlin: Springer)
- [42] Clark B C, Herman R and Wallis R F 1965 *Phys. Rev.* **139** A860
- [43] Matzdorf R *et al* 1996 *Surf. Sci.* **352–354** 670
- [44] Paniago R, Matzdorf R, Meister G and Goldmann A 1995 *Surf. Sci.* **336** 113
- [45] Imada M, Fujimori A and Tokura Y 1998 *Rev. Mod. Phys.* **70** 1039
- [46] Engstrom J R, Tsai W and Weinberg W H 1987 *J. Chem. Phys.* **87** 3104
- [47] Anger G *et al* 1989 *Surf. Sci.* **219** L583
- [48] Greuter F, Strathy I, Plummer E W and Eberhardt W 1986 *Phys. Rev. B* **33** 736
- [49] Rangelov G, Memmel N, Bertel E and Dose V 1990 *Surf. Sci.* **236** 250
- [50] Sandl P, Bischler U and Bertel E 1993 *Surf. Sci.* **291** 29
- [51] Zwick F *et al* 1998 *Phys. Rev. Lett.* **81** 2974
- [52] Fedorov A V *et al* 1999 *Phys. Rev. Lett.* **82** 2179
- [53] Malterre D, Grioni M and Baer Y 1996 *Adv. Phys.* **45** 299
- [54] Matsuura A Y *et al* 1998 *Phys. Rev. B* **58** 3690
- [55] Armitage N P 2003 *Phys. Rev. B* **68** 064517
- [56] Hengsberger M *et al* 1999 *Phys. Rev. Lett.* **83** 592
- [57] Schäfer J *et al* 2004 *Phys. Rev. Lett.* **92** 097205
- [58] Delin A and Tosatti E 2003 *Phys. Rev. B* **68** 144434
- [59] Delin A and Tosatti E 2004 *Surf. Sci.* **566–568** 262
- [60] Redinger S, private communication